Available online at www.sciencedirect.com
SCIENCE DIRECT®
Journal of Theoretical Biology 236 (2005) 39–59
Journal of Theoretical Biology
www.elsevier.com/locate/yjtbi

Post-transplantation dynamics of the immune response to chronic myelogenous leukemia

Rob DeConde[a,1], Peter S. Kim[b,1], Doron Levy[b], Peter P. Lee[c,*]

[a]*Stanford Medical Informatics, Department of Medicine, Stanford University, Stanford, CA 94305, USA*
[b]*Department of Mathematics, Stanford University, Stanford, CA 94305-2125, USA*
[c]*Division of Hematology, Department of Medicine, Stanford University, Stanford, CA 94305, USA*

Received 4 October 2004; received in revised form 24 January 2005; accepted 17 February 2005
Available online 31 March 2005
Communicated by Alan Perelson

Abstract

We model the immune dynamics between T cells and cancer cells in leukemia patients after bone marrow transplants, using a system of six delay differential equations to track the various cell-populations. Our approach incorporates time delays and accounts for the progression of cells through different modes of behavior. We explore possible mechanisms behind a successful cure, whether mediated by a blood-restricted immune response or a cancer-specific graft-versus-leukemia (GVL) effect. Characteristic features of this model include sustained proliferation of T cells after initial stimulation, saturated T cell proliferation rate, and the possible elimination of cancer cells, independent of fixed-point stability. In addition, we use numerical simulations to examine the effects of varying initial cell concentrations on the likelihood of a successful transplant. Among the observed trends, we note that higher initial concentrations of donor-derived, anti-host T cells slightly favor the chance of success, while higher initial concentrations of general host blood cells more significantly favor the chance of success. These observations lead to the hypothesis that anti-host T cells benefit from stimulation by general host blood cells, which induce them to proliferate to sufficient levels to eliminate cancer.

Keywords: Chronic myelogenous leukemia; Immune response; Delayed differential equations; Stem-cell transplant

1. Introduction

Chronic myelogenous leukemia (CML) is a blood cancer with a common acquired genetic defect resulting in the overproduction of abnormal white blood cells. It constitutes nearly 20% of all leukemias, affecting roughly 1 in 100,000 people (Thijsen et al., 1999). Prior to the recent introduction of the drug Gleevec (imatinib or STI571), the life expectancy of CML patients was about 4 years, with only 10% of all patients living beyond 8 years (Cervantes et al., 1994). While these statistics are changing for the better with this new therapy, the requisite large-scale clinical studies have not yet been completed (Tauchi and Ohyashiki, 2004). Gleevec is proving to be effective at controlling CML, but patients still have detectable disease at low levels (Paschka et al., 2003). Allogeneic bone-marrow or stem-cell transplantation (ABMT or ASCT) is the only known curative treatment for CML (Schiffer et al., 2003), and is thus the focus of this work.

There is an abundance of evidence that the immune system plays a critical role in the control of leukemia (Alyea et al., 1998; Bagg, 2002; Marijt et al., 2003; Molldrem et al., 2000; Sawyers et al., 2002; Thijsen et al., 1999), but the exact mechanism of action remains unclear. Infusion of allogeneic donor lymphocytes

*Corresponding author. Tel.: +1 650 498 7942; fax: +1 650 736 0974.
E-mail addresses: rdeconde@smi.stanford.edu (R. DeConde), pkim@math.stanford.edu (P.S. Kim), dlevy@math.stanford.edu (D. Levy), ppl@stanford.edu (P.P. Lee).
[1]Contributed comparably to the paper.

0022-5193/$ - see front matter © 2005 Elsevier Ltd. All rights reserved.
doi:10.1016/j.jtbi.2005.02.015

induces complete cytogenetic response (CR) in 75% of CML patients who relapse after ABMT (Collins et al., 1997; Kolb et al., 1995). The enhanced efficacy of allogeneic over autologous SCT and the potent activity of donor lymphocyte infusion (DLI) have lead to the proposal of a graft-versus-leukemia (GVL) effect, which suggests that the donor lymphocytes mediate the removal of the cancer. Further evidence is found in the correlation between complete remission and both graft-versus-host disease (GVHD) and the loss of chimerism (Kreuzer et al., 2002; Uzunel et al., 2003)—but only when the donor hematopoietic cells prevail as the dominant lineage. Given that GVHD is mediated primarily by T cells, specifically CD8+ cells (Klingebiel and Schlegel, 1998), the above evidence indicates a necessary role for donor T cells in cancer removal.

Researchers have worked to dissect the mechanism by which donor T cells eliminate cancer, with varied results. Marijt et al. (2003) demonstrated that hematopoietic-restricted minor histocompatibility antigens HA-1 and HA-2 can induce a significant response from donor T cells, essentially providing a blood-restricted form of GVHD. Such responses are also associated with the more general form of GVHD (Goulmy et al., 1996). However, since 50% of patients obtain CR without GVHD, it is possible that donor T cells react only against the blood-specific antigens, which may differ between host and donor (Childs et al., 1999; Falkenburg et al., 1999). Thus, leukemia may be eliminated as the result of a more general reaction of the donor T cells against the antigens specific for all host lymphocytes, both cancerous and healthy alike.

Another possible mechanism of GVL is offered by the work of Molldrem et al. (2000), in which they identified T cells that preferentially lysed and inhibited cancer cells over normal marrow cells post-BMT. This work provides evidence that cancer elimination may be governed by a leukemia-specific T-cell response. Neither this cancer-specific mechanism nor the blood-restricted GVHD mechanism are mutually exclusive, and the above studies show that both are possible.

In this work, our goal is to simulate the immune dynamics of a stem-cell transplant in order to elucidate the mechanism of complete remission and to provide insight into potential future therapeutic strategies for treating CML. Our approach is based on following the time evolution of six cell populations: From the donor, we consider anti-cancer T cells (cells specific for leukemia and nothing else), anti-host T cells (those that would mediate a blood-restricted GVHD), and general donor blood cells. From the host, we consider cancer cells, anti-donor T cells (that may be responsible for graft rejection), and general host blood cells. The model is written in terms of a system of delayed differential equations (DDEs), using the delays to account for the progression of cells through various states.

The structure of the paper is as follows. In Section 2 we start with a brief review of the relevant biological and medical background, providing the material upon which the model is based and underlining the importance of the research in this area. We proceed in Section 3 to provide a summary of modeling works in this and related fields, highlighting the strengths of DDEs in this application. Section 4 presents a detailed description of the state diagrams describing the evolution of the various populations through time. We also convert the state diagrams into their entailed DDEs. The various parameters that take part in the model are discussed in Section 5. Our main interest here is the methods for estimating their values. We proceed in Section 6 by demonstrating the results we obtain through numerical simulations of our model. We include examples of relapse, remission, and oscillations. We also analyse the dependence of the long-term outcome on certain parameter values. A discussion of the results is carried in Section 7. Concluding comments that include possible therapeutic strategies are given in Section 8.

2. Biological background

The cause of CML is an acquired genetic abnormality in hematopoietic stem cells in which a reciprocal translocation between chromosomes 9 and 22 occurs. This translocation—creating the Philadelphia (Ph) chromosome—has associated oncogenic properties and can be detected in more than 90% of all patients with CML (Thijsen et al., 1999). Two genes, the tyrosine kinase ABL gene of chromosome 9 and the BCR gene of chromosome 22 combine in the Ph chromosome to form the BCR-ABL fusion gene, driving increased and aberrant tyrosine kinase activity due to this rearrangement. It is this abnormal activity that leads to dysfunctional regulation of cell growth and survival, and consequently to cancer (Thijsen et al., 1999).

The disease traditionally progresses through two or three phases. The first is the chronic phase, in which the cancer grows relatively slowly, the patient shows little or no outward symptoms, and the disease is responsive to therapy. This is followed by a transient accelerated phase, during which the disease accelerates growth and becomes less responsive to therapy. The final and terminal stage of the disease is the blastic phase (or "blast crisis"), during which the disease no longer responds to most therapeutic interventions. In this final phase, the blast count of the patient can rise above 30% and the patient's white blood cell count can climb to levels approaching 300,000 cells per μL (Moore and Li, 2004).

Of all the treatments available to patients, a complete cure is possible only through ASCT. However, this treatment requires a donor with matching human

leukocyte antigens (HLA) and has an associated risk for GVHD, which is the leading cause of treatment-related mortality and morbidity. The risk to the patient is greater for older individuals, and finding a matched donor can be difficult if siblings are unavailable, resulting in the treatment being available to approximately 40% of leukemia patients (Campbell et al., 2001). For the other 60%, there are a number of palliative treatments, including (for some) the milder non-myeloablative stem cell transplant (NST), which involves lower doses of chemotherapy and thus offers an option to older patients (above 60 years old) (Champlin et al., 2000). The fact that this treatment modality involves reduced intensity preparatory regimens of chemotherapy prior to the transplant further highlights the potential of the immune response in controlling leukemia.

ASCT is not always successful, in that even if remission occurs, a patient may still relapse after a period of time. One therapy that has been developed as a response to relapse is DLI, which is designed to reinvigorate or replenish the immune cells that were originally responsible for initiating the original remission (Zorn et al., 2002). Unlike the original transplant, which requires CD8+ cells for GVL efficacy, the DLI can be CD4+ only, and yet a renewal of remission in these cases is still mediated by CD8+ cells (Zorn et al., 2002). It is clear from these results that while CD4+ cells may play a role in GVL, the CD8+ T cells are primarily responsible for cancer removal. There have been speculations as to whether preemptive DLI (infusion before evidence of relapse) could be beneficial, but given that DLI carries with it an associated risk of GVHD, just as the original transplant does, there have been no clinical studies pursuing this hypothesis. It is our hope that the model presented here may be applied to this and other similar questions, where ideas exist that cannot be readily pursued through conventional clinical research.

Treatment and control of CML underwent a dramatic change with the introduction of the new tyrosine kinase inhibitor Gleevec, which has proven to be an effective treatment available to nearly all CML patients, especially in chronic phase (Druker and Lydon, 2000). While 50–60% of patients with advanced-stage CML (blast crisis) also respond to Gleevec, patients are beginning to relapse despite continued therapy (Druker et al., 2001; Sawyers et al., 2002). Furthermore, resistance to Gleevec is becoming recognized in patients in both chronic phase and blast crisis—these have recently been shown to be due to BCR-ABL gene mutation or amplification (Gorre et al., 2001; Shah et al., 2002). Thus, it remains to be seen whether Gleevec represents a true cure for CML and for what percentage of patients, or simply an effective control measure available to be undertaken between or in the place of more aggressive treatments such as ASCT (Campbell et al., 2001).

In order to make ASCT a viable option for more patients and reduce the treatment-associated risks, a number of studies have explored ways of reducing the occurrence of GVHD in ASCT and DLI by altering CD8+ and CD4+ levels in the transplant (Champlin et al., 2000; Klingebiel and Schlegel, 1998; Mutis et al., 1999), with the unfortunate trend that reducing the risk of GVHD (such as reducing CD8+ T-cell levels) incurs a concomitant increase in the chance of relapse. Other works have seen similar results, indicating that the presence of large numbers of mature donor T cells in the stem-cell graft contributes to immune reconstitution and residual leukemia elimination (Drobyski et al., 1994; Godthelp et al., 1999; Horowitz et al., 1990; Sehn et al., 1999; Storek et al., 2001).

3. Modeling background and assumptions

Time-delay differential equation models have been used previously in immune system modeling (Antia et al., 2003), but not as often as the more prevalent ordinary differential equations (ODEs) (Perelson and Weisbuch, 1997). Other alternative approaches include stage-based and agent-based modeling (Chao et al., 2003), each of which offer different trade-offs in computational complexity, whether in high time or population granularity. Time-delay models offer a unique advantage in immune system modeling in that they provide means for dealing with a programmed response. When stimulated by a target, it has been shown that T cells undergo a program of division even if the original stimulation is removed (Chao et al., 2003). Thus, the overall immune response at a given time is not dependent upon the current level of the stimulus, but on the level at some time δ in the past. This can be seen biologically in that peak T cell levels can occur even after complete clearance of antigen (Murali-Krishna et al., 1998).

Regardless of the methods employed, modeling the immune system's interaction with diseases has lead to advances in many fields, the most notable of which is HIV (Essunger and Perelson, 1994; Nowak and May, 2000; Perelson and Nelson, 1999). Among the research pertaining to cancer-related models, Fokas et al. (1991) pioneered modeling CML using non-delay differential equations. More recently, DDE models for immune system and cancer dynamics include Luzyanina et al. (2004) who used a delayed system to describe T cell interactions with lymphocytic choriomeningitis virus (LCMV), and Nelson and Perelson who devised a delay model to examine the influence of antiretroviral drugs on HIV (Nelson and Perelson, 2002). In addition, Villasana and Radunskaya employed DDEs in a model considering tumor cells, immune cells, and a drug interfering with a specific phase of the cell cycle

(Villasana and Radunskaya, 2003). In these papers, the authors use delays to account for the transition times between various stages, such as precursor to effector T cells, uninfected to infected T cells, and interphase to mitosis.

A simple DDE model for the immune response in CML is due to Neiman (2002). This work tried to explain the transition of leukemia from the stable chronic phase to the erratic accelerated and acute phases. In recent work by Moore and Li (2004), they devised a CML model that was composed of a system of ODEs (without delays). Their main goal was to examine which parameters are the most important in influence the success of cancer remission. They concluded that cancer growth and death rates are the most important, and specifically that lower growth rates lead to a greater chance of cancer elimination.

Currently, we only consider CD8+ T cells in our model, since they play the main role in GVHD and leukemia removal. As mentioned previously, while CD4+ cells and other immune cells play important roles in this process, none so much as mature CD8+ cells. Further, previous studies in immune modeling have found that for MHC-I diseases (such as viruses and GVHD), explicit modeling of the separate populations beyond CD8+ or an amalgam of CD4+ and CD8+ has little qualitative effect on the model (Kirschner and Webb, 1996). We also omit explicit modeling of naïve T cells. Given the evidence that production of new naïve T cells requires from 2 to 6 months of thymic recovery post chemotherapy (Dumont-Girard et al., 1998; Roux et al., 2000), the crucial period for GVL seems to occur when naïve cells are in short supply. Further, as our model allows for peripheral expansion of the T cells we include, any effect of naïve cells can be incorporated as a change in the initial conditions.

4. The model

The model tracks the time evolution of six cell populations. From the donor, we consider anti-cancer T cells, anti-host T cells, and all other donor cells (excluding of the two populations explicitly mentioned), denoted by T_C, T_H, and D, respectively. From the host, we consider cancer cells, anti-donor T cells, and general host blood cells, denoted by C, T_D, and H, respectively. The anti-cancer T cells represent the cells that respond to a cancer-specific antigen and exclusively mediate the GVL effect, while the anti-host T cells represent those that respond to a general blood antigen and mediate blood-restricted GVHD.

In the following subsections we present the state diagrams and the corresponding equations for the six populations. The various state diagrams follow the notation shown in Fig. 1. The rectangles stand for the possible states for each population. The arrows represent transitions between states. The terms next to the arrows denote the rates at which cells move from one state to another. Most transitions have an associated time delay indicated by the values in the circles. The values in the circles represent the time it takes to complete the associated transition. Each circle can be thought of as a gate that holds cells in a given state until the appropriate time elapses.

The model only explicitly measures population levels in each of the six base states, one for each cell population. Each term in the equations represents the beginning or the termination of a path connected to the base state (located at or near the center of each state diagram, denoted by the population label). The interaction initiation terms contain no delays, and the rates are proportional to the product of the two interacting populations and a mixing coefficient, k, in accordance with the law of mass action (Moore and Li, 2004). Termination terms contain each rate and delay encountered along their associated paths. Thus, the value of a given population variable, for example T_C, will at times be less than the total number of such cells, because it will not include cells that are within the pipeline of interactions with other populations.

In some cases, a path depicted in the state diagrams will lack an associated term in that population's DDE (for example, the paths to the *Perish* states in the general cell populations D and H, see Section 4.1). This occurs in target cell populations where interactions with T cells that do not lead to death are not included. The motivation lies in the fact that while T cells are limited to one interaction at a time, a target cell may be the subject of scrutiny by several T cells simultaneously, and thus a single interaction is not responsible for removal from the population of available cells.

4.1. General blood cells

The corresponding DDEs for Figs. 2a and b are

$$\frac{dD}{dt} = -d_D D + S_D - p_1^{T_D/D} k D(t-\rho) T_D(t-\rho), \quad (4.1)$$

$$\frac{dH}{dt} = -d_H H + S_H - p_1^{T_H/H} k H(t-\rho) T_H(t-\rho). \quad (4.2)$$

Fig. 2a, shows the state diagram for the general donor blood cells, D. These cells provide stimulus for a graft rejection response from T_D. They play a passive role in all interactions—they do not inspect other cells nor do their behaviors change after interactions, unless they are

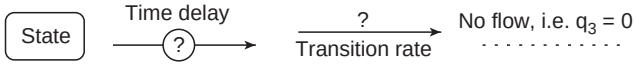

Fig. 1. Symbols in the state diagrams.

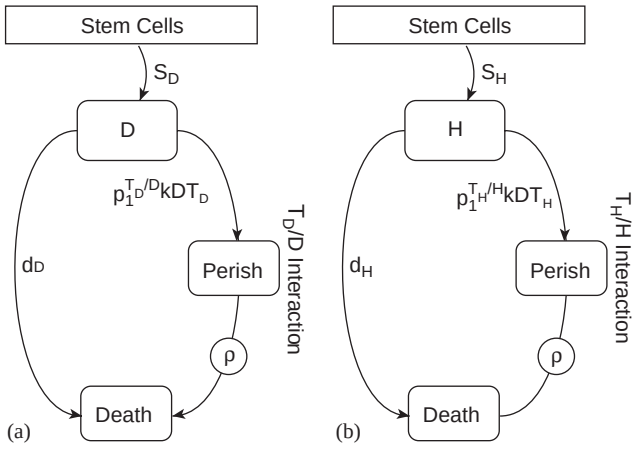

Fig. 2. General donor and host blood cell diagrams.

killed. Consequently, we define D to account for the total concentration in the base state and the *Perish* state.

Donor blood cells move through the state diagram as a result of interactions with T cells, with cells either surviving or perishing depending on the probabilities $p_1^{T_D/D}$ and $p_2^{T_D/D}$. (Here and throughout the paper, we denote probabilities in the form $p_i^{X/Y}$, where X represents the T cell population and Y represents the target cell population involved in the interaction. In other words, X/Y should not be interpreted as an exponent.) Also, stem cells provide a constant flow of new cells, and existing cells die at the natural death rate d_D.

In these and other diagrams, a *Perish* state does not signify that the cell is dead, but rather that the interaction with the given T cell has triggered a cytotoxic response, and that after a time ρ, the cell will be dead as a result.

The general host cells, H, (diagrammed in Fig. 2b) have an analogous role to the donor cells D, in that they provide stimulus for a blood-restricted GVHD response from T_H, and the population has a similar diagram and DDE to the donor population.

4.2. Anti-cancer T cells

Fig. 3 depicts the state diagram for the anti-cancer T cells T_C. The corresponding DDE is

$$\begin{aligned}\frac{dT_C}{dt} = & -d_{T_C}T_C - kCT_C - kT_DT_C \\ & + p_2^{T_C/C}kC(t-\sigma)T_C(t-\sigma) \\ & + p_2^{T_D/T_C}kT_D(t-\sigma)T_C(t-\sigma) + 2^n p_1^{T_C/C}q_1^{T_C/C} \\ & \times kC(t-\rho-n\tau)T_C(t-\rho-n\tau) \\ & + p_1^{T_C/C}q_2^{T_C/C}kC(t-\rho-\upsilon)T_C(t-\rho-\upsilon). \quad (4.3)\end{aligned}$$

These cells interact with two other populations, their target cells C, and the graft-rejecting cells T_D. In the T_C/C interaction (the left wing of Fig. 3) the T cells examine cancer cells and decide whether to react to the stimulus or to ignore it with probabilities $p_1^{T_C/C}$ and $p_2^{T_C/C}$, respectively. If the T cells ignore the stimulus, they return to the base state after a delay of σ, which represents the time for a non-productive interaction. If the T cells react, they have a chance of destroying their targets through a cytotoxic response associated with a delay of ρ. After responding, the cells may enter a cycle of proliferation with probability $q_1^{T_C/C}$. Alternatively, they may forego the proliferation plan and simply recover cytotoxic capabilities (involving the replenishing of cytotoxic granulocytes) in preparation for their next encounter, returning them to the pool of active cells after a delay of υ.

We assume that T cells divide an average of n times during proliferation, resulting in 2^n times as many cells. Each cycle of division takes τ units of time to complete, hence the entire proliferation cycle requires $n\tau$ units of time. We assume that during this time, all proliferating T cells are unavailable to interact with other cells, and thus they are not included in the measure of T_C. When interacting with cancer cells, there is a probability $q_3^{T_C/C}$ that the T cells will become anergic (i.e. tolerant) from the interaction. This effectively amounts to death in our simulations.

The T_D/T_C interaction (the right wing of Fig. 3) represents encounters between anti-cancer cells and anti-donor T cells, where here the T_C cells are only targets. With probability $p_1^{T_D/T_C}$, the T_C cell may perish due to a graft-rejection response from T_D. In addition, some cells die at the natural rate d_{T_C}.

4.3. Anti-host T cells

Fig. 4 shows the state diagram for the anti-host T cells T_H. The corresponding DDE is

$$\begin{aligned}\frac{dT_H}{dt} = & -d_{T_H}T_H - kCT_H - kT_DT_H - kHT_H \\ & + p_2^{T_H/C}kC(t-\sigma)T_H(t-\sigma) \\ & + p_2^{T_D/T_H}p_2^{T_H/T_D}kT_D(t-\sigma)T_H(t-\sigma) \\ & + p_2^{T_H/H}kH(t-\sigma)T_H(t-\sigma) \\ & + 2^n p_1^{T_H/C}q_1^{T_H/C}kC(t-\rho-n\tau)T_H(t-\rho-n\tau) \\ & + 2^n p_1^{T_H/H}q_1^{T_H/H}kH(t-\rho-n\tau)T_H(t-\rho-n\tau) \\ & + 2^n p_2^{T_D/T_H}p_1^{T_H/T_D} \\ & \times q_1^{T_H/T_D}kT_D(t-\rho-n\tau)T_H(t-\rho-n\tau) \\ & + p_1^{T_H/C}q_2^{T_H/C}kC(t-\rho-\upsilon)T_H(t-\rho-\upsilon) \\ & + p_1^{T_H/H}q_2^{T_H/H}kH(t-\rho-\upsilon)T_H(t-\rho-\upsilon) \\ & + p_2^{T_D/T_H}p_1^{T_H/T_D}q_2^{T_H/T_D}kT_D(t-\rho-\upsilon) \\ & \times T_H(t-\rho-\upsilon). \quad (4.4)\end{aligned}$$

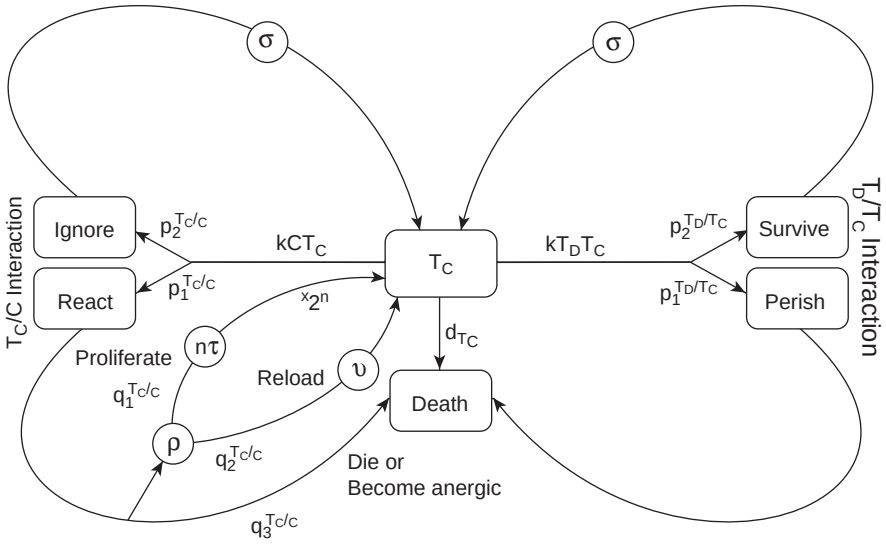

Fig. 3. Anti-cancer T cell diagram.

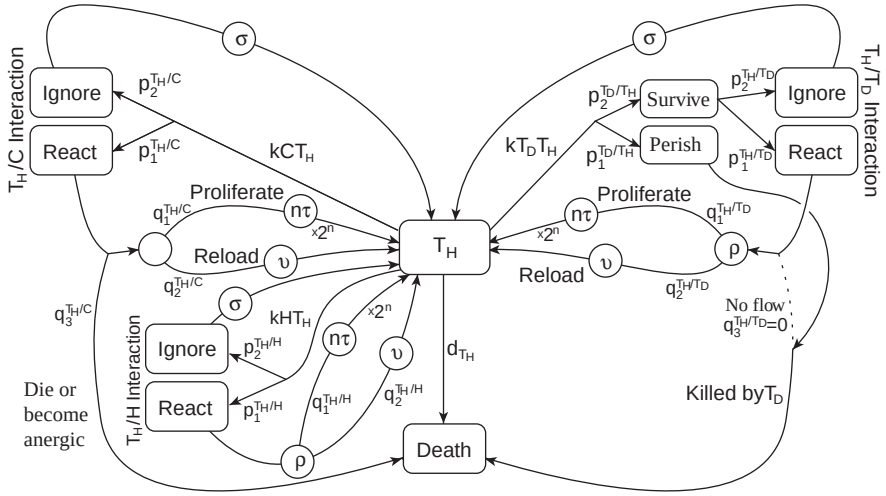

Fig. 4. Anti-host T cell diagram.

This group of cells undergoes interactions with all host cells C, H, and T_D. In the T_H/C interaction (upper left wing of Fig. 4), the anti-host T cells react with cancer in the same way as anti-cancer T cells. In other words, they can either respond to the stimulus or ignore it with probabilities $p_1^{T_H/C}$ and $p_2^{T_H/C}$, respectively. After reacting, there is a probability $q_3^{T_H/C}$ that the T cells will become anergic after the encounter with cancer cells.

In the T_H/H interaction (lower left wing of Fig. 4), the T cells react in the same way with general host blood cells H, except that the general host blood cells cannot cause anergy.

In the T_H/T_D interaction (right wing of Fig. 4), the two types of T cells each have a chance of killing the other. Hence, the probabilities that an anti-host T cell survives the encounter and goes on to react to or ignore its target are $p_2^{T_D/T_H}p_1^{T_H/T_D}$ and $p_2^{T_D/T_H}p_2^{T_H/T_D}$ respectively. The extra factor of $p_2^{T_D/T_H}$ is the probability that the target anti-donor T cell does not kill the anti-host T cell. The remaining anti-host T cells get killed by their interactions with their target anti-donor T cells. Additionally, we assume that although T cells may be killed, they do not become anergic from such interactions. Hence, $q_3^{T_H/T_D}=0$. Some cells also die at a natural death rate d_{T_H}.

4.4. Cancer cells

Fig. 5 depicts the state diagram for the cancer cells C. The corresponding DDE is

$$\frac{dC}{dt} = r_C C(1 - C/m_C) - p_1^{C/T_C} kC(t-\rho)T_C(t-\rho) - p_1^{C/T_H} kC(t-\rho)T_H(t-\rho). \quad (4.5)$$

As target cells, cancer cells have similarly passive roles in interactions to those of D and H, and thus the value of C represents the number of cells in the base state and the two *Perish* states (i.e. all states other than *Death*). In addition, cancer multiplies at a logistic growth rate indicated by the closed loop at the top of the diagram. The logistic parameter r_C represents the net growth rate of cancer, which includes its natural death rate, and the parameter m_C represents the carrying capacity of the cancer population.

The C/T_H and C/T_C interactions are analogous to the T_D/D and T_H/H interactions for the general blood cells in Section 4.1.

4.5. Anti-donor T cells

Fig. 6 depicts the state diagram for the anti-donor T cells, T_D. The corresponding DDE is

$$\begin{aligned}\frac{dT_D}{dt} &= -d_{T_D}T_D - kT_CT_D - kT_HT_D - kDT_D \\ &\quad + p_2^{T_D/T_C}kT_C(t-\sigma)T_D(t-\sigma) \\ &\quad + p_2^{T_H/T_D}p_2^{T_D/T_H}kT_H(t-\sigma)T_D(t-\sigma) \\ &\quad + p_2^{T_D/D}kD(t-\sigma)T_D(t-\sigma) \\ &\quad + 2^n p_1^{T_D/T_C}q_1^{T_D/T_C}kT_C(t-\rho-n\tau)T_D(t-\rho-n\tau) \\ &\quad + 2^n p_2^{T_H/T_D}p_1^{T_D/T_H} \\ &\quad \times q_1^{T_D/T_H}kT_H(t-\rho-n\tau)T_D(t-\rho-n\tau) \\ &\quad + 2^n p_1^{T_D/D}q_1^{T_D/D}kD(t-\rho-n\tau)T_D(t-\rho-n\tau) \\ &\quad + p_1^{T_D/T_C}q_2^{T_D/T_C}kT_C(t-\rho-\upsilon)T_D(t-\rho-\upsilon) \\ &\quad + p_2^{T_H/T_D}p_1^{T_D/T_H}q_2^{T_D/T_H}kT_H(t-\rho-\upsilon)T_D(t-\rho-\upsilon) \\ &\quad + p_1^{T_D/D}q_2^{T_D/D}kD(t-\rho-\upsilon)T_D(t-\rho-\upsilon). \end{aligned} \tag{4.6}$$

The anti-donor T cells respond to anti-cancer T cells T_C, general donor blood cells D, and anti-host T cells T_H the same way anti-host T cells respond to C, H, and T_D, respectively. Hence, the diagram for anti-donor T cells is analogous to the one for anti-host T cells in Fig. 4. The only difference is that we assume anti-cancer T cells cannot cause anergy in anti-donor T cells, so $q_3^{T_D/T_C} = 0$ on the lower right wing of Fig. 6. Similarly, $q_3^{T_D/T_H} = 0$ on the lower left wing.

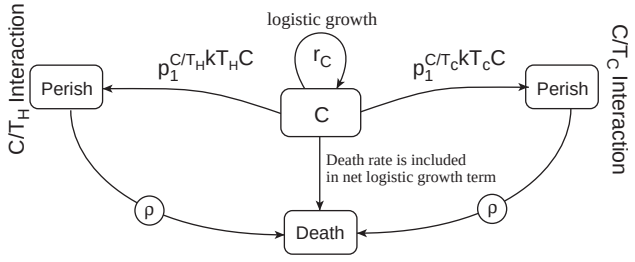

Fig. 5. Cancer diagram.

5. Parameters

5.1. Setting the parameters

The various parameters used in our model are summarized in Tables 1 and 2. Whenever possible, we obtained their values directly from the literature, although at times we had to make do with estimation when specific information was unavailable.

The delays ρ, σ, τ, and υ come from known values for these events and interactions (see Table 1 for references). For the death rates, if we use the conservative estimate that T cells have a half life of about three days without stimulation (Duvall and Perry, 1968), then the T cell

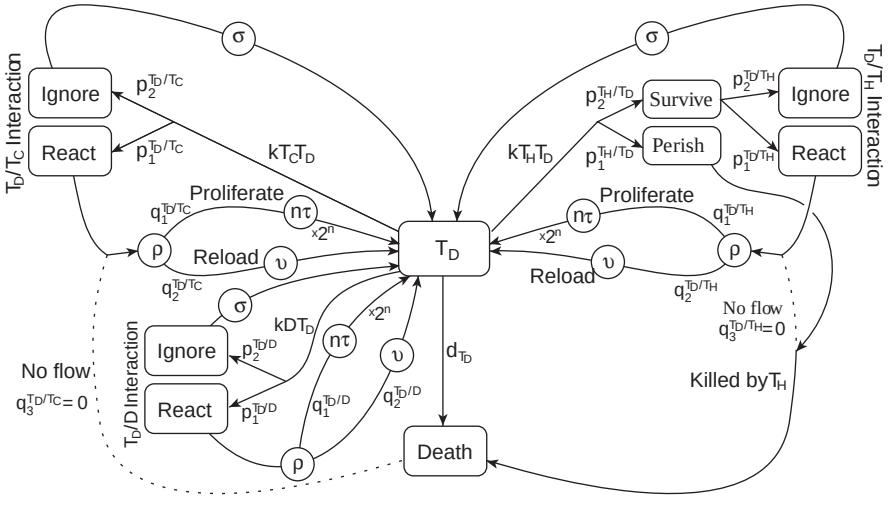

Fig. 6. Anti-donor T cell diagram.

death rates d_{T_C}, d_{T_H}, and d_{T_D} are about $0.23\,\text{day}^{-1}$. If we assume that general cells have a half life of about a week, the death rates d_H and d_D are about $0.10\,\text{day}^{-1}$.

The cancer growth rate for the Gompertz function is estimated in Moore and Li (2004) to be 0.03, while several studies (Fokas et al., 1991; Stryckmans et al., 1977) report that cancer cells multiply at the same rate, or perhaps more slowly, than normal myeloid cells at a rate of 0.9% per week during the chronic phase. Assuming exponential growth, this observation yields an estimated net growth rate of $(\ln 1.009)/(7\,\text{days}) = 0.0013\,\text{day}^{-1}$. In our model, we use a logistic function, but nonetheless, we can estimate that the logistic cancer growth rate r_C has an order of magnitude around 10^{-2} and 10^{-3}.

The precise number of programmed cell divisions a mature T cell undergoes after stimulation was not

Table 1
Parameters

Param.	Description	Estimate	References
Delays (day)			
ρ	Time for reactive T cell-antigen interactions	0.0035 (5 min)	(Friedl and Gunzer, 2001)
σ	Time for unreactive interactions	0.0007 (1 min)	(Friedl and Gunzer, 2001)
τ	Time for cell division	0.5–1.5	(Chao et al., 2003; Lee, Unpublished data)
υ	T cell recovery time after killing another cell	1	(Friedl and Gunzer, 2001)
Growth and death rates (day^{-1})			
d_{T_C}, d_{T_H}, d_{T_D}	T cell death rates	0.23	(Duvall and Perry, 1968)
d_D, d_H	General death rate	0.1	Estimated
r_C	Net cancer growth rate	$10^{-3}-10^{-2}$	(Fokas et al., 1991; Moore and Li, 2004; Stryckmans et al., 1977)
m_C	Logistic carrying capacity for cancer	$1.5-3.5\times10^5$ (cells/μL)	Estimated
n	Avg # of T cell divisions after stimulation	<8 times	(Antia et al., 2003)
Proportionality constant for law of mass action $(\text{cells}/\mu\text{L})^{-1}\,\text{day}^{-1}$			
k	Kinetic mixing rate	10^{-3}	(Luzyanina et al., 2004)

Table 2
Transition probabilities[a]

Param.	Description	Estimate
Probabilities		
$p_1^{X/Y}$	Probability of a reactive X/Y interaction	$p_1^{X/Y}+p_2^{X/Y}=1$
$p_2^{X/Y}$	Probability of an unreactive X/Y interaction	
$q_1^{X/Y}$	Probability that X proliferates after interaction	$q_1^{X/Y}+q_2^{X/Y}+q_3^{X/Y}=1$
$q_2^{X/Y}$	Probability that X keeps probing after interaction	
$q_3^{X/Y}$	Probability that X becomes anergic after interaction	
$p_1^{T_H/H}$, $p_1^{T_H/T_D}$, $p_1^{T_D/D}$, $p_1^{T_D/T_C}$, $p_1^{T_D/T_H}$		0.9
$p_1^{T_C/C}$, $p_1^{T_H/C}$		0.8
p_1^{C/T_C}, p_1^{C/T_H}		0.6
$q_i^{T_H/H}$, $q_i^{T_H/T_D}$, $q_i^{T_D/D}$, $q_i^{T_D/T_C}$, $q_i^{T_D/T_H}$		0.5 ($i=1,2$)
$q_i^{T_C/C}$, $q_i^{T_H/C}$		0.25 ($i=1,2$)

[a]Estimates based on observed patient data.

directly available, despite ample evidence that such peripheral expansion takes place (Godthelp et al., 1999; Horowitz et al., 1990; Storek et al., 2001). Using population-wide expansion and estimates for naïve T cell proliferation (Antia et al., 2003), we set the average number of effector cell divisions n to be less than or equal to 8.

The theoretical limit for the number of white blood cells in the blood is about 3.5×10^5 cells/μL, and healthy white blood cells rarely exceed $5-10 \times 10^3$ cells/μL. However, in reality, the cancer cell level often saturates at around 1.5×10^5 cells/μL, so we estimate the carrying capacity for cancer m_C to be between 1.5 and 3.5×10^5 cells/μL (Lee, Unpublished data).

The kinetic mixing coefficient k is an elusive kinetic parameter, which we compare to the rate constant of virus elimination in Luzyanina et al. (2004) to obtain the ballpark estimate of 10^{-3} (cells/μL)$^{-1}$ day^{-1}.

The probabilities denoted by p depend on the cross-reactivities of the interacting populations, and the probabilities denoted by q depend on how the cells proceed after reactive interactions (see Table 2). In addition, the parameters of the form p_1 depend on the antigenicity of the target, which we assume is high for most interactions. Consequently, we set $p_1^{T_H/H}$ and $p_1^{T_D/D}$ equal to 0.9. This value may be lower for interactions between two T cells, but for simplicity, we also set $p_1^{T_D/T_C}$, $p_1^{T_H/T_D}$, and $p_1^{T_D/T_H}$ equal to 0.9. The probabilities of the forms q_1 and q_2 govern whether or not the cells start to proliferate after stimulation, or simply recover cytotoxic capability in preparation for their next encounter. For now, we assume $q_1 = q_2$ in all cases.

For T cell-cancer interactions, we have the following assumptions (Lee, Unpublished data): 20% of the time nothing happens, and both cells survive and depart; 20% of the time cancer lives, and the T cell becomes anergic or dysfunctional; 40% of the time cancer dies, and the T cell survives and moves on; 20% of the time both cancer and the T cell die. From these assumptions, we can deduce the following probabilities: the probability of a reactive interaction is 0.8; the probability that the T cell dies is 0.4; and the probability that cancer dies is 0.6. The values above correspond to the probabilities $p_1^{T_C/C}, p_1^{T_C/C} q_3^{T_C/C}$, p_1^{C/T_C}. If as before we assume $q_1^{T_C/C} = q_2^{T_C/C}$, then the p's and q's are uniquely determined and listed in Table 2. We also use the same values for the corresponding T_H/C and C/T_H probabilities.

5.2. Initial concentrations and stem cell supply rates

The initial concentrations and stem cell levels are summarized in Table 3.

Table 3
Initial concentrations[a]

Param.	Description	Estimate
Initial concentrations (cells/μL)		
$T_{C,0}$	Anti-cancer T cells	$10^{-1}-1$
$T_{H,0}$	Anti-host T cells	$10^{-1}-1$
D_0	General donor cells	$\leqslant 10^3$
C_0	Cancer cells	$< 1.7 \times 10^{-3}$
$T_{D,0}$	Anti-donor T cells	$\ll 1.7 \times 10^{-4}$
H_0	General host cells	$\leqslant 10$
Stem cell supply rates ((cells/μL) day^{-1})		
S_D	Donor cell resupply rate	$10^{-6}-10^{-5}$
S_H	Host cell resupply rate	$10^{-8}-10^{-7}$

[a]Estimates derived from patient data from the Blood and Marrow Transplantation Division of the Stanford Medical School.

Prior to an allogeneic bone marrow transplant (ABMT), a patient receives intense chemotherapy and possibly radiation to reduce the cancer load, which has the added effect of depleting the host immune system. If remission is achieved, the cancer load has reached levels undetectable by reverse transcriptase polymerase chain reaction (RT-PCR), which has a sensitivity to about 10^4 cells in the body (Bagg, 2002). Considering that the average person has about 6 L of blood, this number yields a cancer cell concentration of less than $10^4/6\,\text{cells/L} = 1.7 \times 10^{-3}$ cells/μL after treatment. In addition, the patient's healthy white blood cell count makes up less than a tenth of the total healthy and unhealthy white blood cell count, and only a small fraction of these represent functioning CD8+ T cells that could react against donor cells (Lee, Unpublished data). Thus, we make the following estimates: initial cancer concentration $C_0 < 1.7 \times 10^{-3}$ cells/μL and initial anti-donor T cell concentration $T_{D,0} \ll 1.7 \times 10^{-4}$ cells/μL.

Furthermore, the intense chemotherapy also greatly reduces the host's hematopoietic stem cell (HSC) population. As we will calculate in the following paragraph, the HSC count is about one-fiftieth the T cell count. In addition, we estimate the division rate of stem cells to be close to the growth rate of cancer, which is 0.01 day^{-1}. This means that the supply rate, S_H, of new host cells is about $T_{D,0}/50 \times 0.01\,\text{day}^{-1} \ll 3.4 \times 10^{-8}$ (cells/μL) day^{-1}. Hence, for our estimate, we assume that the supply rate, S_H, is on the order of $10^{-11}-10^{-10}$ (cells/μL) day^{-1}.

During the past 5 years, HSC have been obtained by giving the donor a drug that causes stem cells to mobilize from his or her bone marrow and circulate in the bloodstream. At this time, the donor's blood is collected in an apheresis machine and analysed for

the CD34+ marker. Currently this marker is the best detection method, but still only 1 in 10,000 to 1 in 100,000 CD34+ cells is a true HSC. The collection continues until the sample reaches a target total number of CD34+ cells, which usually ranges from 2.4 to 10×10^6 CD34+ cells per kg of the recipient's body weight. For a standard (full intensity chemotherapy) ABMT, the patient typically receives 3×10^6 CD34+ cells per kg. For a non-myeloablative (reduced intensity chemotherapy) ABMT, the patient receives 5×10^6 CD34+ cells per kg. Finally, the collected product generally contains 0.1% to 1% CD34+ cells and 30% to 50% T cells.

We also make use of the following information (Lee, Unpublished data):

1. A healthy adult has a blood concentration of about 1×10^3 cells/μL of CD4+ T cells and 6×10^2 cells/μL of CD8+ T cells. Hence, the ratio of CD8+ T cells to total T cells is $600/1600 = 0.375$.
2. The body contains approximately 6.7×10^{11} naïve T cells with about 2.5×10^7 different specificities (Arstila et al., 1999). Each T cell expresses one TCR specificity that responds to about 100 or more different peptide-MHC (pMHC) complexes at different levels of cross-reactivity (Valmori et al., 2000). A cancer cell contains on the order of 10,000 genetic events, some of which lead to unique peptide antigens (Stoler et al., 1999). Assuming 1% of the genetic events lead to new antigens which stimulate 100 TCR configurations with 50% cross-reactivity, we obtain $10,000 \times 1\% \times 100 \times 50\% = 5000$ tumor-reactive T cell specificities. So, out of the entire naïve T cell population, we expect about $5000/(2.5 \times 10^7) = 1/5000$ naïve T cells to be tumor-reactive. To calculate our initial values, we assume that this frequency estimate for naïve T cells carries over to effector T cells.

In addition, we assume that on average a person weighs 75 kg and has 6 L of blood. We denote the concentration of any quantity x by $[x]$. Based on our assumption, the various values for the collected bone marrow transplant can be computed as follows:

$$[\text{CD34+}] = \frac{75\,\text{kg} \times (3 \times 10^6 \text{CD34+/kg})}{6\,\text{L}} = 3.5 \times 10^7\,\text{cells/L},$$

$$[\text{HSC}] = [\text{CD34+}] \times (10^{-5} - 10^{-4}\,\text{HSC/CD34+}) = 3.5 \times 10^{-4} \text{ to } 10^{-3}\,\text{cells/μL},$$

$$\frac{\text{T cells}}{\text{CD34+ cells}} = \frac{30-50\%}{0.1-1\%} = 30-500,$$

$$[\text{T cell}] = [\text{CD34+}] \times (30-500) = 1.05-17.5 \times 10^3\,\text{cells/μL}, \quad (5.1)$$

$$[\text{Tumor reactive T cell}] = \frac{c(\text{T cell})}{5000} = 0.21-3.5\,\text{cells/μL},$$

$$[\text{Tumor reactive CD8+}] = [\text{Tumor reactive T cell}] \times 0.375-10^{-1} \text{ to } 10^0\,\text{cells/μL}. \quad (5.2)$$

Using the estimate that the division rate of stem cells is $0.01\,\text{day}^{-1}$, we obtain that the supply rate, S_D, of new donor cells is about $\text{HSC} \times 0.01\,\text{day}^{-1} = 3.5 \times 10^{-6}$ to $10^{-5}\,(\text{cells/μL})\,\text{day}^{-1}$. In addition, the value for the tumor reactive CD8+ T cell concentration (5.2) corresponds to the sum of the initial anti-cancer and anti-host T cell concentrations $T_{C,0} + T_{H,0}$.

The initial concentrations of residual host and donor blood cells, H_0 and D_0, cannot be measured easily, because these populations include numerous types of blood cells. Furthermore, chemotherapy and irradiation deplete the residual host blood cells to levels below the detection limit of about 10 cells/μL.[2] Hence, we can only make the rough estimate that the initial residual host blood cell concentration, H_0, is below 10 cells/μL. To estimate the initial residual donor blood cell concentration, D_0, we assume that the ratio between D_0 and H_0 is approximately the same as the ratio between the corresponding stem cell levels, which is $S_D/S_H \sim 10^{-6}/10^{-8} = 10^2$. Hence, we estimate that D_0 is around or below $10\,\text{cells/μL} \times 10^2 = 10^3\,\text{cells/μL}$.

In our simulations, we choose $D_0 = 1000\,\text{cells/μL}$ and H_0 to be on the order of 1 cell/μL, because this range of parameters allows us to inspect the behavior in regions where the model makes transitions between parameter regions where cancer relapse occurs to regions where complete remission occurs.[3]

[2] We discussed the more sensitive method of RT-PCR for detecting leukemic cells at the beginning of Section 5.2. However, RT-PCR relies on a unique oncogene or translocation (e.g. BCR-ABL) in certain leukemic cells, which would not be available for residual host blood cells. Hence, the detection limit for residual host blood cells is much higher than the RT-PCR limit of 10^{-3} cells/μL.

[3] The influence of the parameter D_0 on the model is insignificant for any value around or less than 1000 cells/μL. However, the results are highly sensitive to the value of H_0 for H_0 around 1 cell/μL. For H_0 much less than 1 cell/μL, cancer nearly always relapses, and for H_0 much greater than 1 cell/μL, cancer is almost always eliminated. This trend is discussed more fully in Section 6.5.

6. Numerical simulations and results

6.1. Jump start adjustment

In delay differential equations, the values of the variables for $t<0$ must be set as an initial condition. To obtain the most meaningful initial conditions for our model, we assume the host cell populations to be at a steady state before the transplant, while the donor-derived cell populations are not present until the time of the transplant at $t=0$. In other words, the values up to time 0 are denoted by the vector $[T_{C,0}\delta(t), T_{H,0}\delta(t), D_0\delta(t), C_0, T_{D,0}, H_0]$, where the terms $T_{C,0}$, $T_{H,0}$, D_0, C_0, $T_{D,0}$, and H_0 denote the concentrations of the six cell populations at time 0, and

$$\delta(t)=\begin{cases}0 & \text{if } t\neq 0,\\ 1 & \text{if } t=0.\end{cases}$$

6.2. State constraint

The model incorporates negative terms with positive delays in the three target-cell populations (cancer, host, and donor cells), which can cause the values of these populations to pass through zero and become negative. (Note that this phenomenon would not occur with the corresponding ODEs without the delays.) This is a result of target availability, where target cells are not removed from the available population when an interaction is initiated with a T cell. Instead, they wait until a cytotoxic event before leaving, which allows a slight overestimation of T cell efficacy. While more biologically accurate, target availability requires a correction for the associated artifact, which comes in the form of the state constraint that a population's derivative must remain nonnegative when that population value reaches zero. For example with the general donor blood cell population, D, because of the delay, ρ, in the expression for $\mathrm{d}D/\mathrm{d}t$ (Eq. (4.1)), the term $\mathrm{d}D/\mathrm{d}t$ might still be negative even though $D(t)=0$, since the term $D(t-\rho)$ might be positive. To account for this artifact, we set

$$\mathrm{d}D/\mathrm{d}t=\begin{cases}\text{the value from Eq.(4.1)} & \text{if } D(t)>0,\\ \text{the positive part of that value} & \text{if } D(t)=0.\end{cases}$$

We apply the same state constraint to all other populations. Note that for the cancer population, the value from Eq. (4.5) is always less than or equal to zero when $C(t)=0$. Hence, the state constraint becomes

$$\mathrm{d}C/\mathrm{d}t=\begin{cases}\text{the value from Eq. (4.5)} & \text{if } C(t)>0,\\ 0 & \text{if } C(t)=0.\end{cases}$$

Furthermore, for the three T cell populations, T_C, T_H, and T_D, the values from Eqs. (4.3), (4.4), and (4.6) are always nonnegative when T_C, T_H, and T_D equal zero. Hence, the state constraint is not supposed to come into play. Nevertheless, to account for possible errors from numerical approximations, we apply the state constraint to all six cell populations when running simulations.

In our numerical simulations, it is quite possible that extinction may result from numerical artifacts due to the error of approximation. Even so, in practice, once a modeled population passes below a certain threshold, some authors consider it extinct due to minute fluctuations and noise (which we do not include in the model).

6.3. Extinction instead of stability

In all our numerical simulations we use the 'dde23' delay-differential equation solver in MATLAB 6.5. We took the relative and absolute tolerances for numerical approximations to be MATLAB's default values of 10^{-3} and 10^{-6}, respectively. We found that for much lower tolerances, such as 10^{-6} and 10^{-9}, it becomes much less likely for the cancer cell population to reach zero in the numerical simulations. Hence, by applying the default values, we have implicitly imposed a tolerance governing when we consider a numerical quantity to be effectively at zero.

From the definition of $\mathrm{d}C/\mathrm{d}t$ and the state constraint discussed above, if the cancer concentration ever hits zero, it remains there and does not recover. Hence, the event $C(t)=0$ implies total cancer elimination, which serves as a natural criterion for a successful cure. On the other hand, if we remove the state constraint, the cancer population may become negative and give rise to an unstable oscillation as shown in Fig. 7(*left*).

Therefore, for the purposes of this model, we study the conditions that lead to the extinction of the cancer population rather than the stability of cancer-free fixed points. We find this choice appropriate, since in our case, unstable oscillations around a cancer-free fixed point will cause some populations' values to travel below zero and back. At this point, the values are not biologically meaningful and probably imply the complete elimination of one or more or the cell populations. Indeed, in Luzyanina et al. (2004, p. 11), made the same observation in their model when they noted that very large oscillations are not biologically realistic, and therefore imply the elimination of the virus.

An additional difficulty with stability analysis for this model is that the characteristic equations associated with the DDEs are transcendental, as one would expect. Hence, the eigenvalues are very difficult to analyse, especially since the model incorporates four different delays: ρ, σ, $\rho+n\tau$, and $\rho+\upsilon$.

In light of the extinction criterion, the solution of the DDEs would behave very differently if we removed the delay ρ. Specifically, the cancer population would never reach zero. Indeed, if we set $\rho=0$, then

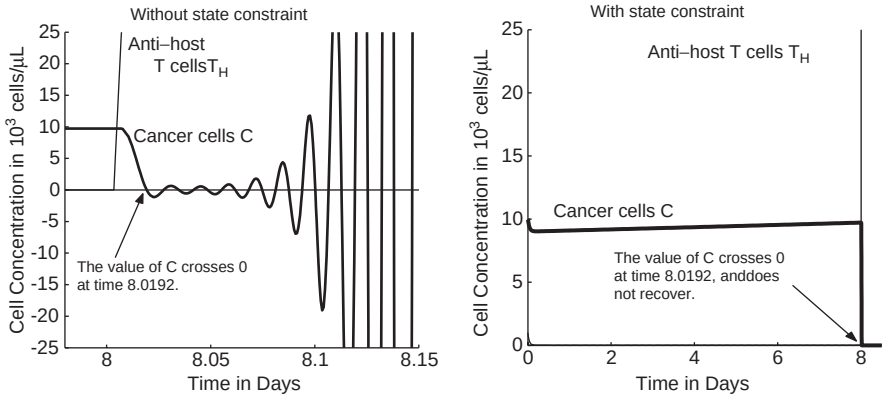

Fig. 7. Effect of the state constraint. (left) Without a state constraint. (right) With a state constraint (see Appendix A for parameters).

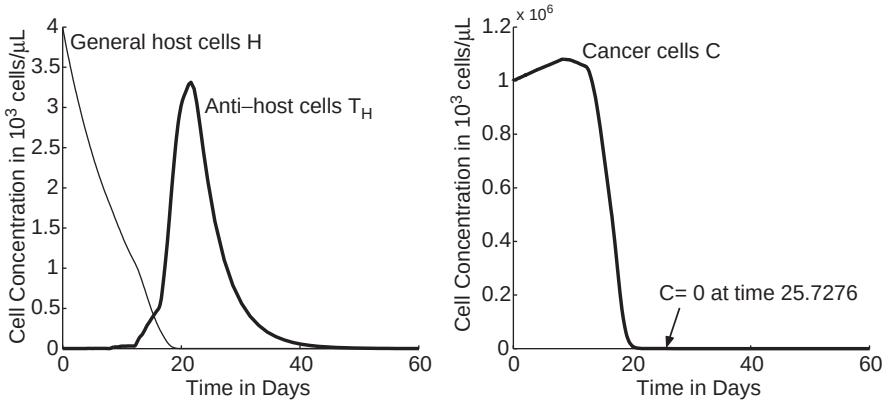

Fig. 8. Complete remission (see Appendix A for parameters).

Eq. (4.5) would be

$$\frac{dC}{dt} = \{r_C(1 - C/m_C) - p_1^{C/T_C} k T_C(t) - p_1^{C/T_H} k T_H(t)\} C, \tag{6.1}$$

and a derivative of this form would not allow the value of C to ever become 0. Hence, despite the fact that ρ is on a much smaller time-scale than the other delays τ and υ, its presence is essential for our analysis. For consistency, we also include the delay σ which is on the same time-scale as ρ.

6.4. Representative examples

A notable characteristic of the state-based delay model is the delayed T cell response to antigen stimulation. Due to the time lag, T cells continue to proliferate even after the stimulus disappears. This phenomenon occurs because of a delayed feedback loop, such as the one discussed in Bernard et al. (2003). In particular, the delay for T cell proliferation is $n\tau$, so the primed T cells withdraw for $n\tau$ units of time and divide n times regardless of what happens to the stimulus in between. This behavior follows the notion of an antigen-independent T cell proliferation program described in Antia et al. (2003). Essentially, the delayed reaction gives T cells the momentum to effectively and thoroughly remove the target.

In this model, when the T cell response works effectively, the donor-derived T cells, T_C and T_H, can quickly and completely stamp out cancer cells after an initial delay. This is shown in Fig. 8.

From Fig. 8, it appears that the anti-host T cell concentration T_H suddenly jumps at 4, 8, 12, and 16 days after the transplant. Zooming in on this region we see the jumps more clearly in Fig. 9, (*left* and *center*). These jumps occur because T_H represents the subpopulation of anti-host T cells that are available for interaction, not the entire population. Most of the anti-host T cells react to general host blood cells or cancer cells shortly after time 0; these cells withdraw and divide for $n = 4$ cycles, which last roughly 4 days. After this period, these T cells return to the available population after having multiplied $2^4 = 16$ times over. These cycles of withdrawal and proliferation continue in intervals lasting about 4 days, and as time goes on the

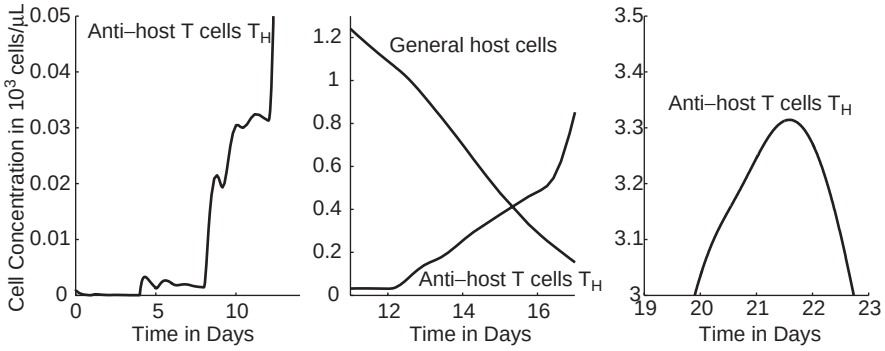

Fig. 9. Rescaled version of Fig. 8 (see Appendix A for parameters).

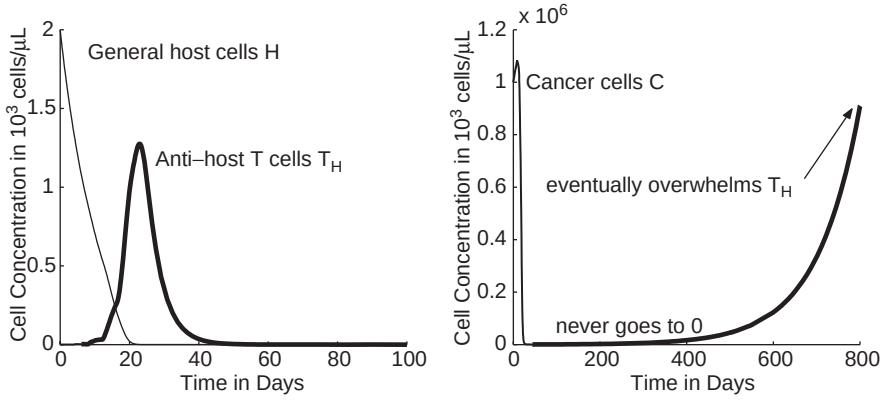

Fig. 10. Relapse (see Appendix A for parameters).

jumps become more attenuated and spread out. Notably, the sudden drops in the net cancer growth rate coincide in time with the jumps in available anti-host T cells. In reality, the total anti-host T cell population, including those that are dividing, increases more smoothly than the population represented by T_H, but for the purposes of the model, we only need to keep track of available T cells. As another characteristic feature of the model, the anti-host T cell peak occurs after about 21.5 days (Fig. 9, *right*), which is about a day later than when the cancer population steeply drops off.

If the T cells do not completely destroy the cancer, relapse occurs. In this situation, the cancer remains well below detectable levels for a period of time, due to the slow growth rate $r \sim 10^{-2}$, before returning and overwhelming the depleted T cell population. This is shown in Fig. 10.

For a narrow range of parameters, one can also obtain several cycles of oscillations before cancer ultimately dies out or relapses. This is shown in Fig. 11. The occurrence of oscillations in the model is rare, but corroborates the occurrence of Jeff's phenomenon, where tumor levels have been observed to fluctuate around a fixed point (Villasana and Radunskaya, 2003, p. 285).

6.5. Behavioral trends

Figs. 12–16 depict results from multiple simulations in which we varied two parameters while holding all others fixed. These results show how the behavior of the model changes across different parameter ranges. We apply the following criteria to automatically determine whether a parameter set leads to a cure by a specified time t:

- Successful: Cancer count goes to 0, i.e. $C(t) \leqslant 0$.
- Unsuccessful: T cells are exhausted, and cancer relapses to near carrying capacity, i.e. $T_C(t) \leqslant 0$, $T_H(t) \leqslant 0$, and $C(t) \geqslant 1.5 \times 10^5$ cells/μL.
- Unresolved: Neither of the above hold.

This method of varying parameters in pairs allows us to look at general trends with relatively modest computational time. Another useful approach is Latin Hypercube Sampling. For example, in Moore and Li (2004), Moore and Li apply Latin Hypercube Sampling to a different model of leukemia and determine that the likelihood of cancer remission decreases as cancer growth rate increases. However, due to the large number of parameters in our model, such an analysis would greatly increase the computation time and is not

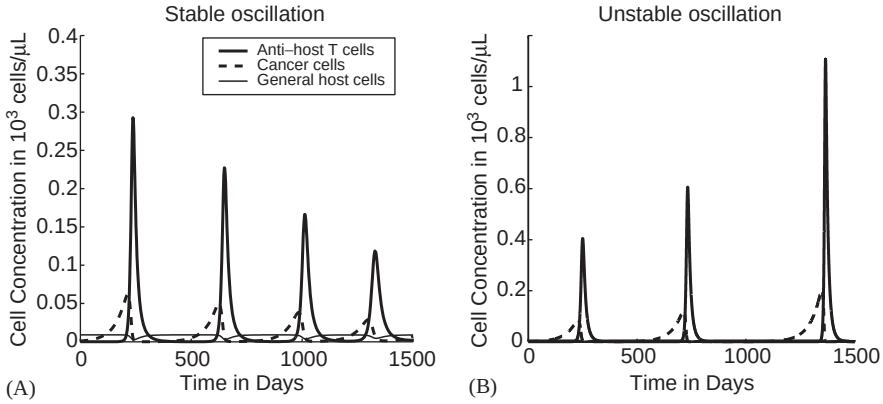

Fig. 11. Oscillations (see Appendix A for parameters).

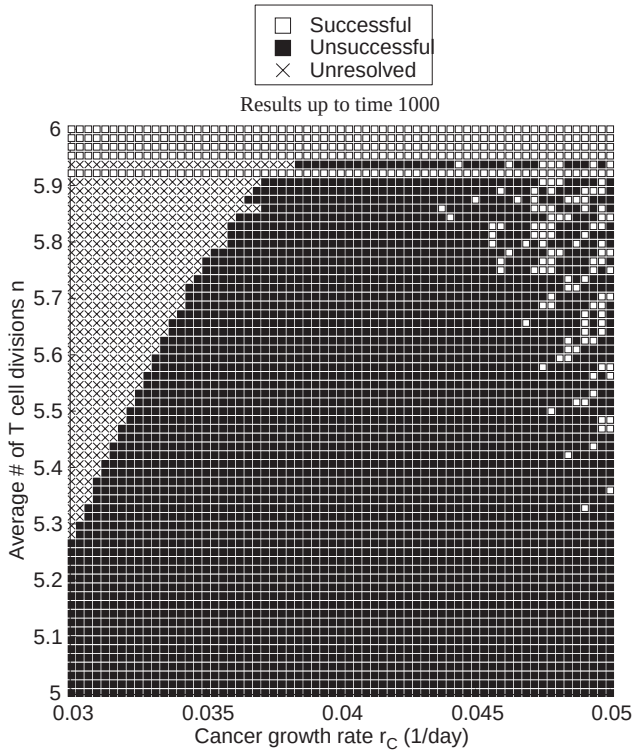

Fig. 12. r_C vs. n (see Appendix A for parameters).

necessary to observe the qualitative trends that we seek to obtain.

In the five examples in Figs. 12–16, we vary the parameter pairs: r_C vs. n; H_0 vs. n; $T_{D,0}$ vs. $T_{H,0}$; H_0 vs. $T_{H,0}$; and H_0 vs. r_C, respectively, with a focus on the transition regions where the global behavior of the model changes according to the criteria outlined above. Each of these parameters was selected due to its potential accessibility via therapeutic treatment (H_0 for example, can be modulated by varying the intensity of the chemotherapy preparatory regimen). The values of the constant parameters are reported in Appendix A.

We summarize the behavioral trends apparent from these graphs in items 1 through 5 below. We note that in nearly all cases, the anti-cancer T cells (T_C) die out very quickly due to an initial lack of stimulation from the low levels of cancer immediately following chemotherapy, a point we include as item 6.

1. Higher cancer growth rates r_C make complete remission slightly more likely after a bone marrow transplant. (Figs. 12–16)
2. Higher average numbers of T cell division after stimulation favor complete remission. (Figs. 12 and 13)
3. Anti-donor T cells T_D usually die off, but a high initial level $T_{D,0}$ can cripple the donor T cell levels and prevent a successful transplant. (Fig. 14)
4. Higher initial host blood cell concentrations H_0 greatly improve the chances of a successful cure. (Figs. 13, 15 and 16)
5. Greater initial anti-host T cell concentrations $T_{H,0}$ slightly favor the chances of a cure, but less so than with high initial host blood cell concentrations H_0. (Fig. 15)
6. Cancer-specific T cells T_C usually die out quickly and do not affect the success of a transplant.

In the grids, we observe that the boundaries between successful and unsuccessful regions is not smooth and there are occasional, aberrant points in the middle of otherwise homogeneous regions. These results are not surprising, since we applied an extinction criterion rather than a stability criterion to differentiate between success and failure. These results show that conditions for complete cancer extinction are very sensitive to parameters and initial cell concentrations. However, despite its sensitivity, the grids also indicate clear trends in behavior as certain parameters are varied. We use these trends to form several hypotheses that we elaborate below.

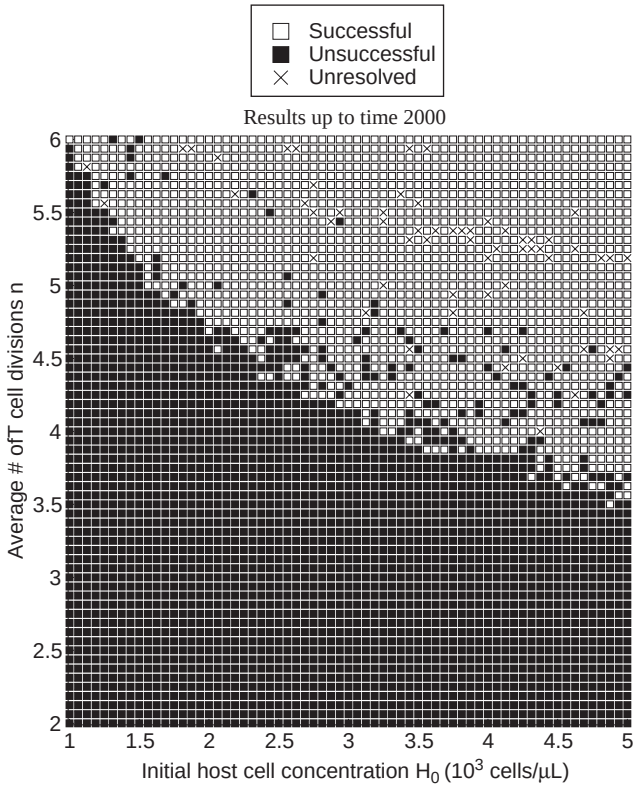

Fig. 13. H_0 vs. n (see Appendix A for parameters).

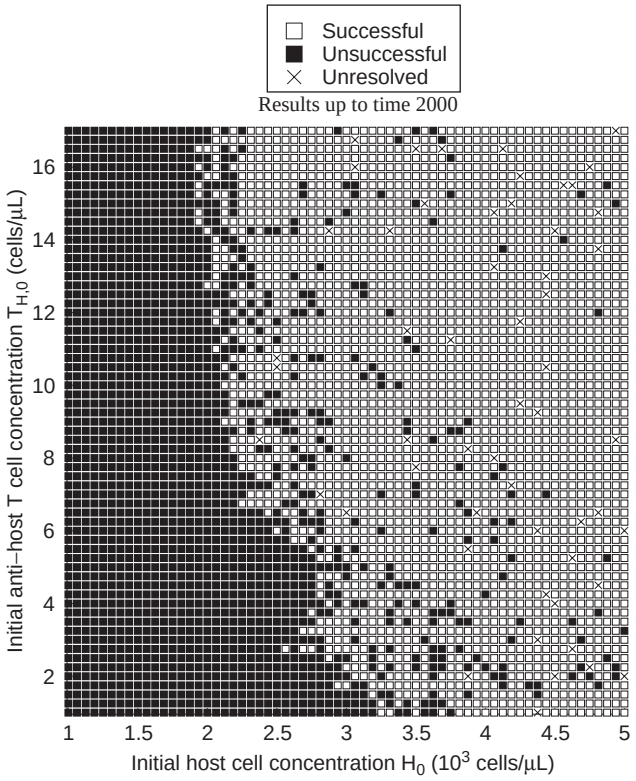

Fig. 15. H_0 vs. $T_{H,0}$ (see Appendix A for parameters).

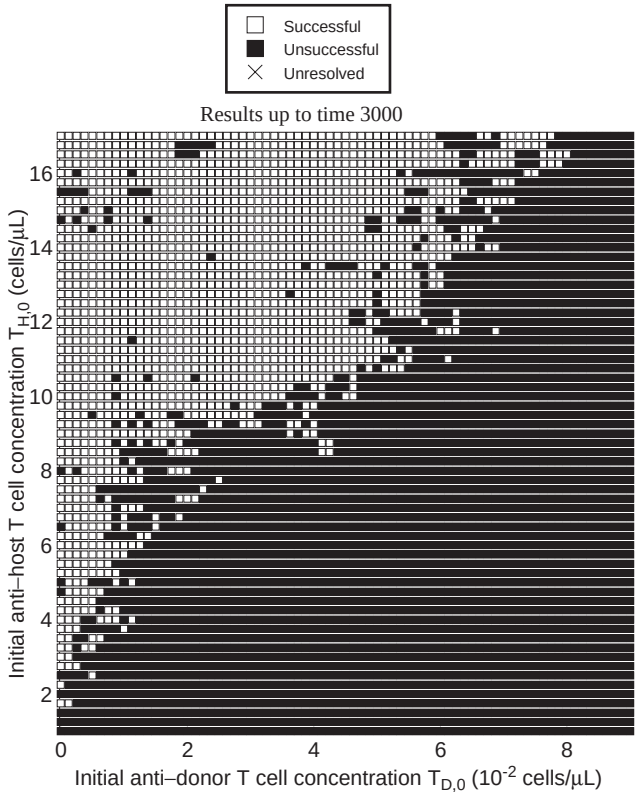

Fig. 14. $T_{D,0}$ vs. $T_{H,0}$ (see Appendix A for parameters).

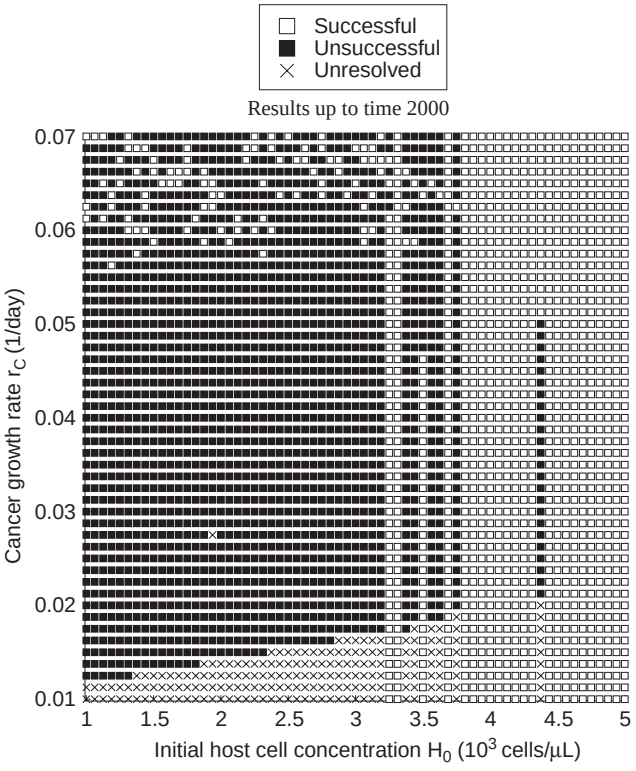

Fig. 16. H_0 vs. r_C (see Appendix A for parameters).

7. Discussion

This model presents a novel approach to simulating cell interactions by using delays to capture the transitions between modes of behavior. The method extends ideas from the comprehensive non-delay differential equation model of Moore and Li (2004) and the simpler delay-based model of Neiman (2002), incorporating added biological and mathematical features over these previous works.

In our model, T cells reach a maximum proliferation rate without the use of a Michaelis–Menten or similar correction term. For example, T cells cannot multiply faster than $2^n/(\rho + n\tau)$ times per day, and this maximum is attained only if the relevant transition rates are all infinite. Hence, the delays naturally capture the sequential nature of interactions and the saturation effects due to time lags, features which often require artificial corrections in ODE models and others lacking delays.

Any model will have its set of accompanying assumptions and corrections. Specifically, the state constraint (see Section 6.2) necessitated by target availability deserves future exploration. The artifact may, in fact, be less accurate than the removal of this feature. As an alternative, we could treat the target cells in the same way as the T cells in that they are completely removed from the interacting populations during cell-to-cell encounters. In this case, the state constraint would not be necessary, but the cancer population would never completely reach extinction. A thorough exploration of such a possibility will accompany future iterations of the model. Furthermore, additional biological features arguably should be considered. For example, separating the T cell population into CD4+ and CD8+ compartments, and each of these compartments into naïve, effector, and memory subsets, are some of the modifications that could be incorporated into the model. These features may not be necessary for the present application of the model, but will be required to explore findings that specifically pertain to these cell populations (Alyea et al., 1998; Shedlock and Shen, 2003; Sun and Beven, 2003; Zorn et al., 2002).

7.1. Discussion of behavior

The behavior of the cell populations in this model generally falls into three categories: complete cancer remission, cancer relapse, and oscillation followed by either remission or relapse. Examples of these types of behavior are shown in Figs. 8, 10, and 11, respectively.

Although the model incorporates six populations, most populations are transient and die out after 30 to 60 days. Since chemotherapy depletes the initial levels of anti-donor T cells, T_D, these T cells start at very low levels and are usually overwhelmed by anti-host T cells. In addition, chemotherapy also greatly reduces the cancer cell population, so the anti-cancer T cells T_C, which lack the proxy stimulus of the general host cells in addition to cancer, are without sufficient initial stimulus to drive a significant response and prevent extinction. Thus, they die out quickly and are usually depleted before the cancer relapses. While this does not eliminate the possibility of a cancer-specific GVL effect, it suggests that there is insufficient stimulus for such a mechanism, and by implication the dominant means of cancer removal is blood-restricted GVHD (see point 6 in Section 6.5).

Despite the transient nature of roughly half the cell populations, they all can influence the result of a complete remission or relapse. For example, the general host blood cells H provide the necessary stimulus for the anti-host T cells T_H to start proliferating. Thus, their initial level is very important even though they typically die out within 30 days. In their absence, the level of cancer is too low to initiate a proper response alone. In addition, the anti-donor T cells have the potential to substantially attenuate the anti-host T cell proliferation response, because anti-donor T cells can destroy anti-host T cells. Hence, a high initial population of anti-donor T cells may cause the anti-host T cell response to be inadequate to completely remove the cancer. Each of these counterbalancing measures offers a potential opportunity for therapeutic intervention to tip the scales in favor of complete remission. (See the Conclusion section for further discussion of such possibilities.)

7.2. Discussion of trends

The first point in Section 6.5 offers what may seem to be a counter-intuitive result, indicating that clinical outcome is actually improved with a higher cancer growth rate post-ASCT, in the presence of an immune response. When cancer grows quickly, it initiates a larger T cell response (assuming the appropriate population has not already gone extinct) and thus it is more likely to be cleared from the host. In contrast, a slow growth rate may either allow T cell populations enough time to diminish significantly, or may lead to stable or unstable oscillations. Two biological phenomena that are not explicitly included in the model can aid in interpreting this result. First, inclusion of memory cells would help prevent the T cell population from dropping beyond certain thresholds. However, except for narrow parameter ranges, their overall effect is to transform T cell extinction situations into damped oscillations (unpublished data). With inclusion of the second phenomena, anergy, we can interpret such oscillations as eventual relapse as the T cells slowly acquire tolerance due to the repeated exposure to the target cells.

Thus, slower cancer growth leads to a higher chance of relapse. This finding is supported by biological

observations that leukemia cells proliferate no faster than normal progenitor cells (Clarkson and Strife, 1993; Strife et al., 1988). The observation also coincides with the prediction of Luzyanina et al. (2004, p. 7). In their model of LCMV, they predict that the virus can persist at low levels, if the replication rate of the virus is smaller than it was during acute infection.

On the other hand, this result contrasts the conclusion of Moore and Li (2004) that lower cancer growth rates favor cancer elimination. However, in their model, they examined the dynamics of cancer and immune cell interaction within the patient's body without an ABMT. They utilize Michaelis–Menten corrections throughout their model, in addition to Gompertz law. At the same time, their saturation point for cancer is significantly higher (three orders of magnitude) than for the T cells. Thus, increased growth rate for cancer will always be beneficial for cancer persistence as long as it can grow beyond the saturation point of the T cells, which are capped in their stimulus response regardless of how fast cancer grows. In contrast, while our model incorporates saturating rates of change due to delays, we did not place an absolute cap on the T cell population, relying on the cap included for cancer as a surrogate for the T cells. A future model may need to incorporate both delays and absolute population caps (beyond just cancer), to elucidate the details underlying these differing results.

For the second point, we notice that as the average number of T cell divisions n after stimulation increases, the chance of a complete remission also increases. Indeed, for greater values of n, the T cell response takes more time to ramp up, but it ultimately reaches higher levels, which aid in the successful removal of cancer.

The third point supports the expected notion that the host immune system reacts against the donor bone marrow and can cause an unsuccessful transplant. Since the anti-donor T cell concentration starts at low levels as estimated in Section 5, these cells nearly always dwindle to extinction. However, their initial levels significantly affect the likelihood of a successful cure. This point is in accordance with the treatment procedure that a patient must go through chemotherapy and irradiation to deplete his or her immune system prior to the bone marrow transplant, in order to avoid graft rejection.

Points 4 and 5 provide a strong evidence that higher initial general host blood cell concentrations, H_0, strongly improve the chances of a successful cure. The anti-host T cells proliferate to high levels in response to the large stimulus (from both general host and cancer cells), which enable them to eliminate the cancer in a blood-restricted GVHD response. It is worth noting that there is an associated risk with such a response of incurring general GVHD (see Section 1), and the model, at present, makes no attempt to incorporate it. Future work will likely need to include this detail, as the results suggest that providing further stimulation for such a blood-restricted GVHD response may be a promising method of increasing the likelihood of a sustained remission.

The fifth observation speaks to the efficacy of DLI. The results indicate that while increasing effector cell concentrations will have a positive effect on cancer removal, the magnitude will be much less than if target cell concentrations are raised. We will explore this point further in the Conclusion.

The sixth point implies that a general blood-restricted immune response is a much more likely mechanism for a successful cure than a cancer-specific GVL effect. This point corroborates points 4 and 5 by showing that a certain level of additional stimulus from general host blood cells is not only beneficial, but even necessary for a successful cure.

8. Conclusion

This DDE model, simulating conditions in CML post-transplant, indicates a higher sensitivity to increased target cells than increased T cells. At present, DLI is a standard treatment for patients that relapse after a stem cell transplant, which for the purpose of our model provides an increase in T_H. While this does have a positive effect in eliminating the resurgent cancer, both within our model and biologically, our model suggests a novel treatment strategy: it may be more effective to infuse host cells, thus raising H and driving a stronger antigen response. These infusions would require prior irradiation or some other treatment to prevent the reintroduction of viable cancer cells, but may carry a lower risk of initiating GVHD, since this would mainly drive a blood-restricted immune response.

The timing of the infusion is also important in eliminating cancer. As discussed in Section 1, an open treatment question is whether preemptive DLI (before any evidence of a relapse) would be beneficial, reasoning that it may be better to go after the remaining cancer before waiting for a relapse. One problem with this approach is that there is no way to know a priori which patients will relapse and which are already cured, and hence some healthy patients will be subjected to the risks associated with an unnecessary procedure. We have already mentioned the potentially reduced risk of infusing host cells over donor cells, but in addition, the model indicates that a preemptive DLI using standard donor cells will be less effective than waiting for a relapse. This derives from the antigen driven response, where if the level of cancer is sufficiently low to be cytogenetically undetectable (as with patients in relapse), it will provide no supportive stimulus to the infused cells. Thus, the infusion will dwindle and die with only a small probability of locating and eliminating all of the few remaining cancer cells. In contrast,

infusion of proxy cells that stimulate or maintain a blood-restricted GVHD response can keep the effector-cell-to-cancer ratio high for extended periods of time, maximizing the probability that the cancer will be eliminated.

These hypotheses require both further modeling of the specific scenarios described as well as an evaluation of the biological validity of the theories. However, already the model has provided insights into possible new directions for CML treatment and research, in addition to demonstrating some of the benefits of utilizing DDEs as a modeling tool in immunology.

Acknowledgements

The work of Doron Levy was supported in part by the NSF under Career Grant DMS-0133511. The work of Peter S. Kim was supported by the NSF Graduate Research Fellowship Program and the Department of Mathematics at Stanford University. We would also like to acknowledge the Blood and Marrow Transplantation Division of the Stanford Medical School for providing us with parameters derived from CML patients who underwent allogenic bone marrow transplantation. The work of Peter P. Lee was supported in part by the American Cancer Society Research Scholar Grant and the Stanford Office of Technology Licensing Incentive Award.

Appendix A. Parameters for figures

Parameters for figures are given below (Table 4).

Table 4
Parameters for figures

Parameter	Value							
Figure #	7	8, 10	11A, B	12	13	14	15	16
ρ	0.0035	0.0035	0.0035	0.0035	0.0035	0.0035	0.0035	0.0035
σ	0.0007	0.0007	0.0007	0.0007	0.0007	0.0007	0.0007	0.0007
τ	1	1	1	1	1	1	1	1
υ	1	1	1	1	1	1	1	1
$p_1^{T_H/H}$, $p_1^{T_H/T_D}$, $p_1^{T_D/D}$, $p_1^{T_D/T_C}$, $p_1^{T_D/T_H}$	1	0.9	0.9	0.9	0.9	0.9	0.9	0.9
$p_1^{T_C/C}$, $p_1^{T_H/C}$	1	0.8	0.9	0.8	0.8	0.8	0.8	0.8
p_1^{C/T_C}, p_1^{C/T_H}	1	0.6	0.9	0.6	0.6	0.6	0.6	0.6
$q_1^{T_H/H}$, $q_1^{T_H/T_D}$, $q_1^{T_D/D}$, $q_1^{T_D/T_C}$, $q_1^{T_D/T_H}$	1	0.5	0.5	0.5	0.5	0.5	0.5	0.5
$q_2^{T_H/H}$, $q_2^{T_H/T_D}$, $q_2^{T_D/D}$, $q_2^{T_D/T_C}$, $q_2^{T_D/T_H}$	0	0.5	0.5	0.5	0.5	0.5	0.5	0.5
$q_1^{T_C/C}$, $q_1^{T_H/C}$,	1	0.25	0.5	0.25	0.25	0.25	0.25	0.25
$q_2^{T_C/C}$, $q_2^{T_H/C}$	0	0.25	0.5	0.25	0.25	0.25	0.25	0.25
d_{T_C}, d_{T_H}, d_{T_D}	0.23	0.23	0.1	0.23	0.23	0.23	0.23	0.23
d_D, d_H	0.1	0.1	0.1	0.1	0.1	0.1	0.1	0.1
r_C	0.01	0.01	0.02	varies	0.02	0.02	0.02	varies
m_C	2×10^5	2×10^5	2×10^5	2×10^5	2×10^5	2×10^5	2×10^5	2×10^5

Table 4 (*continued*)

Parameter	Value							
Figure #	7	8, 10	11A, B	12	13	14	15	16
n	8	4	4	varies	varies	4	4	4
k	0.003	0.001	0.001	0.001	0.001	0.001	0.001	0.001
$T_{C,0}$	0	0	0	1	1	1	1	1
$T_{H,0}$	1000	1	0.1	1	1	varies	varies	1
D_0	0	0	0	1000	1000	1000	1000	1000
C_0	10^4	0.001	1	0.001	0.001	0.001	0.001	0.001
$T_{D,0}$	0	0	0	1×10^{-5}	1×10^{-5}	varies	1×10^{-5}	1×10^{-5}
H_0	0	**4**, **2**	**9**, **6**	1	varies	3	varies	varies
S_D	0	0	0	10^{-5}	10^{-5}	10^{-5}	10^{-5}	10^{-5}
S_H	0	0	**9**, **6** $\times 10^{-1}$	10^{-7}	10^{-7}	10^{-7}	10^{-7}	10^{-7}

References

Alyea, E.P., Soiffer, R.J., Canning, C., Neuberg, D., Schlossman, R., Pickett, C., Collins, H., Wang, Y., Anderson, K.C., Ritz, J., 1998. Toxicity and efficacy of defined doses of CD4+ donor lymphocytes for treatment of relapse after allogeneic bone marrow transplant. Blood 19 (10), 3671–3680.

Antia, R., Bergstrom, C.T., Pilyugin, S.S., Kaech, S.M., Ahmed, R., 2003. Models of CD8+ responses: 1. What is the antigen-independent proliferation program. J. Theor. Biol. 221 (4), 585–598.

Arstila, T.P., Casrouge, A., Baron, V., Even, J., Kanellopoulos, J., Kourilsky, P., 1999. A direct estimate of the human alphabeta T cell receptor diversity. Science 286 (5441), 958–961.

Bagg, A., 2002. Chronic myeloid leukemia: a minimalistic view of post-therapeutic monitoring. J. Mol. Diagn. 4 (1), 1–10.

Bernard, S., Belair, J., Mackey, M.C., 2003. Oscillations in cyclical neutropenia: new evidence based on mathematical modeling. J. Theor. Biol. 223 (3), 283–298.

Campbell, J.D., Cook, G., Holyoake, T.L., 2001. Evolution of bone marrow transplantation—the original immunotherapy. Trends Immunol. 22 (2), 88–92.

Cervantes, F., Robertson, J.E., Rozman, C., Baccarani, M., Tura, S., Gomez, G.A., Braun, T.J., Clarkson, B.D., Pereira, A., 1994. Long-term survivors in chronic granulocytic leukaemia: a study by the International CGL Prognosis Study. Group, Italian Cooperative CML Study Group. Br. J. Haematol. 87, 293–300.

Champlin, R., Khouri, I., Shimoni, A., Gajewski, J., Kornblau, S., Molldrem, J., Ueno, N., Giralt, S., Anderlini, P., 2000. Harnessing graft-versus-malignancy: non-myeloablative preparative regimens for allogeneic haematopoietic transplantation, an evolving strategy for adoptive immunotherapy. Br. J. Haematol. 111 (1), 18–29.

Chao, D.L., Forrest, S., Davenport, M.P., Perelson, A.S., 2003. Stochastic stage-structured modeling of the adaptive immune system. Proceedings of the Computational Systems Bioinformatics.

Childs, R., Epperson, D., Bahceci, E., Clave, E., Barrett, J., 1999. Molecular remission of chronic myeloid leukaemia following a non-myeloablative allogeneic peripheral blood stem cell transplant: in vivo and in vitro evidence for a graft-versus-leukaemia effect. Br. J. Haematol. 107 (2), 396–400.

Clarkson, B., Strife, A., 1993. Linkage of proliferative and maturational abnormalities in chronic myelogenous leukemia and relevance to treatment. Leukemia 7 (11), 1683–1721.

Collins Jr., R.H., Shpilberg, O., Drobyski, W.R., Porter, D.L., Giralt, S., Champlin, R., Goodman, S.A., Wolff, S.N., Hu, W., Verfaillie, C., List, A., Dalton, W., Ognoskie, N., Chetrit, A., Antin, J.H., Nemunaitis, J., 1997. Donor leukocyte infusions in 140 patients with relapsed malignancy after allogeneic bone marrow transplantation. J. Clin. Oncol. 15 (2), 433–444.

Drobyski, W.R., Ash, R.C., Casper, J.T., McAuliffe, T., Horowitz, M.M., Lawton, C., Keever, C., Baxter-Lowe, L.A., Camitta, B., Garbecht, F., et al., 1994. Effect of T-cell depletion as graft-versus-host disease prophylaxis on engraftment, relapse, and disease-free survival in unrelated marrow transplantation for chronic myelogenous leukemia. Blood 83, 1980–1987.

Druker, B.J., Lydon, N.B., 2000. Lessons learned from the development of an ABL tyrosine kinase inhibitor for chronic myelogenous leukemia. J. Clin. Invest. 105 (1), 3–7.

Druker, B.J., Sawyers, C.L., Kantarjian, H., Resta, D.J., Reese, S.F., Ford, J.M., Capdeville, R., Talpaz, M., 2001. Activity of a specific inhibitor of the BCR-ABL tyrosine kinase in the blast crisis of chronic myeloid leukemia and acute lymphoblastic leukemia with the Philadelphia chromosome. N. Engl. J. Med. 344 (14), 1038–1042.

Dumont-Girard, F., Roux, E., van Lier, R.A., Hale, G., Helg, C., Chapuis, B., Starobinski, M., Roosnek, E., 1998. Reconstitution of the T-cell compartment after bone marrow transplantation: restoration of the repertoire by thymic emigrants. Blood 92 (11), 4464–4471.

Duvall, C.P., Perry, S., 1968. The use of 51-chromium in the study of leukocyte kinetics in chronic myelocytic leukemia. J. Lab. Clin. Med. 71, 614–628.

Essunger, P., Perelson, A.S., 1994. Modeling HIV infection of CD4+ T-cell subpopulations. J. Theor. Biol. 170, 367–391.

Falkenburg, J.H., Wafelman, A.R., Joosten, P., Smit, W.M., van Bergen, C.A., Bongaerts, R., Lurvink, E., van der Hoorn, M., Kluck, P., Landegent, J.E., Kluin-Nelemans, H.C., Fibbe, W.E., Willemze, R., 1999. Complete remission of accelerated phase chronic myeloid leukemia by treatment with leukemia-reactive cytotoxic T lymphocytes. Blood 94 (4), 1201–1208.

Fokas, A.S., Keller, J.B., Clarkson, B.D., 1991. Mathematical model of granulocytopoiesis and chronic myelogenous leukemia. Cancer Res. 51, 2084–2091.

Friedl, P., Gunzer, M., 2001. Interaction of T cells with APCs: the serial encounter model. Trends Immunol. 22 (2), 187–191.

Godthelp, B.C., van Tol, M.J., Vossen, J.M., van Den Elsen, P.J., 1999. T-cell immune reconstitution in pediatric leukemia patients after allogeneic bone marrow transplantation with T-cell-depleted or unmanipulated grafts: evaluation of overall and antigen-specific T-cell repertoires. Blood 94, 4358–4369.

Gorre, M.E., Mohammed, M., Ellwood, K., Hsu, N., Paquette, R., Rao, P.N., Sawyers, C.L., 2001. Clinical resistance to STI-571 cancer therapy caused by BCR-ABL gene mutation or amplification. Science 293 (5531), 876–880.

Goulmy, E., Schipper, R., Pool, J., Blokland, E., Falkenburg, J.H., Vossen, J., Gratwohl, A., Vogelsang, G.B., van Houwelingen, H.C., van Rood, J.J., 1996. Mismatches of minor histocompatibility antigens between HLA-identical donors and recipients and the development of graft-versus-host disease after bone marrow transplantation. N. Engl. J. Med. 334 (5), 281–285.

Horowitz, M.M., Gale, R.P., Sondel, P.M., Goldman, J.M., Kersey, J., Kolb, H.J., Rimm, A.A., Ringden, O., Rozman, C., Speck, B., Truitt, R.L., Zwaan, F.E., Bortin, M.M., 1990. Grafte-versus-leukemia reaction after bone marrow transplantation. Blood 75, 555–562.

Kirschner, D., Webb, G.F., 1996. A model for treatment strategy in the chemotherapy of AIDS. Bull. Math. Biol. 58 (2), 367–390.

Klingebiel, T., Schlegel, P.G., 1998. GVHD: overview on pathophysiology, incidence, clinical and biological features. Bone Marrow Transplant 21 (Suppl. 2), S45–S49.

Kolb, H.J., Schattenberg, A., Goldman, J.M., Hertenstein, B., Jacobsen, N., Arcese, W., Ljungman, P., Ferrant, A., Verdonck, L., Niederwieser, D., et al., 1995. Graft-versus-leukemia effect of donor lymphocyte transfusions in marrow grafted patients, European group for blood and marrow transplantation working party chronic leukemia. Blood 86 (5), 2041–2050.

Kreuzer, K.-A., Schmidt, C.A., Schetelig, J., Held, T.K., Thiede, C., Ehninger, G., Siegert, W., 2002. Kinetics of stem cell engraftment and clearance of leukaemia cells after allogeneic stem cell transplantation with reduced intensity conditioning in chronic myeloid leukaemia. Eur. J. Haematol. 69, 7–10.

Lee, P.P., Unpublished data.

Luzyanina, T., Engelborghs, K., Ehl, S., Klenerman, P., Bocharov, G., 2004. Low level viral persistence after infection with LCMV: a quantitative insight through numerical bifurcation analysis. Math. Biosci. 173, 1–23.

Marijt, W.A.E., Heemskerk, M.H.M., Kloosterboer, F.M., Goulmy, E., Kester, M.G.D., van der Hoorn, M.A.W.G., van Luxemburg-Heys, S.A.P., Hoogeboom, M., Mutis, T., Drijfhout, J.W., van Rood, J.J., Willemze, R., Falkenburg, J.H.F., 2003. Hematopoiesis-restricted minor histocompatibility antigens HA-1- or HA-2-specific T cells can induce complete remissions of relapsed leukemia. Proc. Natl Acad. Sci. 100 (5), 2742–2747.

Molldrem, J.J., Lee, P.P., Wang, C., Felio, K., Kantarjian, H.M., Champlin, R.E., Davis, M.M., 2000. Evidence that specific T lymphocytes may participate in the elimination of chronic myelogenous leukemia. Nat. Med. 6 (8), 1018–1023.

Moore, H., Li, N.K., 2004. A mathematical model for chronic myelogenous leukemia (CML) and T cell interaction. J. Theor. Biol. 227, 513–523.

Murali-Krishna, K., Altman, J.D., Suresh, M., Sourdive, D.J.D., Zajac, D.J.D., Miller, J.D., Slansky, J., Ahmed, R., 1998. Counting antigen-specific CD8+ T cells: a re-evaluation of bystander activation during viral infection. Immunity 8, 177–187.

Mutis, T., Gillespie, G., Schrama, E., Falkenburg, J.H., Moss, P., Goulmy, E., 1999. Tetrameric HLA class I-minor histocompatibility antigen peptide complexes demonstrate minor histocompatibility antigen-specific cytotoxic T lymphocytes in patients with graft-versus-host disease. Nat. Med. 5, 839–842.

Neiman, B., 2002. A Mathematical Model of Chronic Myelogenous Leukemia. M.Sc. Dissertation, University College, Oxford University, UK.

Nelson, P.W., Perelson, A.S., 2002. Mathematical analysis of delay differential equation models of HIV-1 infection. Math. Biosci. 179, 73–94.

Nowak, M.A., May, R.M., 2000. Virus Dynamics. Oxford University Press, Oxford, UK.

Paschka, P., Muller, M.C., Merx, K., Kreil, S., Schoch, C., Lahaye, T., Weisser, A., Petzold, A., Konig, H., Berger, U., Gschaidmeier, H., Hehlmann, R., Hochhaus, A., 2003. Molecular monitoring of response to imatinib (Glivec) in CML patients pretreated with interferon alphs. Low levels of residual disease are associated with continuous remission. Leukemia 17 (9), 1687–1694.

Perelson, A.S., Nelson, P.W., 1999. Mathematical analysis of HIV-I dynamics in vivo. SIAM Rev. 41 (1), 3–44.

Perelson, A.S., Weisbuch, G., 1997. Immunology for physicists. Rev. Mod. Phys. 69 (4), 1219–1267.

Roux, E., Dumont-Girard, F., Starobinski, M., Siegrist, C.-A., Helg, C., Chapuis, B., Roosnek, E., 2000. Recovery of immune reactivity after T-cell-depleted bone marrow transplantation depends on thymic activity. Blood 96 (6), 2299–2303.

Sawyers, C.L., Hochhaus, A., Feldman, E., Goldman, J.M., Miller, C.B., Ottmann, O.G., Schiffer, C.A., Talpaz, M., Guilhot, F., Deininger, M.W., Fischer, T., O'Brien, S.G., Stone, R.M., Gambacorti-Passerini, C.B., Russell, N.H., Reiffers, J.J., Shea, T.C., Chapuis, B., Coutre, S., Tura, S., Morra, E., Larson, R.A., Saven, A., Peschel, C., Gratwohl, A., Mandelli, F., Ben-Am, M., Gathmann, I., Capdeville, R., Paquette, R.L., Druker, B.J., 2002. Imatinib induces hematologic and cytogenetic responses in patients with chronic myelogenous leukemia in myeloid blast crisis: results of a phase II study. Blood 99 (10), 3530–3539.

Schiffer, C.A., Hehlmann, R., Larson, R., 2003. Perspectives on the treatment of chronic phase and advanced phase CML and Philadelphia chromosome positive ALL. Leukemia 17, 691–699.

Sehn, L.H., Alyea, E.P., Weller, E., Canning, C., Lee, S., Ritz, J., Antin, J.H., Soiffer, R.J., 1999. Comparative outcomes of T-cell-depleted and non-T-cell-depleted allogeneic bone marrow transplantation for chronic myelogenous leukemia: impact of donor lymphocyte infusion. J. Clin. Oncol. 17, 561–568.

Shah, N.P., Nicoll, J.M., Nagar, B., Gorre, M.E., Paquette, R.L., Kuriyan, J., Sawyers, C.L., 2002. Multiple BCR-ABL kinase domain mutations confer polyclonal resistance to the tyrosine kinase inhibitor imatinib (STI571) in chronic phase and blast crisis chronic myeloid leukemia. Cancer Cell 2 (2), 117.

Shedlock, D.J., Shen, H., 2003. Requirement for CD4 T cell help in generating functional CD8 T cell memory. Science 300, 337–339.

Stoler, D.L., Chen, N., Basik, M., Kahlenberg, M.S., Rodriguez-Bigas, M.A., Petrelli, N.J., Anderson, G.R., 1999. The onset and extent of genomic instability in sporadic colorectal tumor progression. Proc. Natl Acad. Sci. USA 96 (26), 15121–15126.

Storek, J., Dawson, M.A., Storer, B., Stevens-Ayers, T., Maloney, M.G., Marr, K.A., Witherspoon, R.P., Bensinger, W., Flowers, M.E.D., Martin, P., Storb, R., Appelbaum, F.R., Boeckh, M., 2001. Immune reconstitution after allogeneic marrow transplantation compared with blood stem cell transplantation. Blood 97 (11), 3380–3389.

Strife, A., Lambek, C., Wisniewski, D., Wachter, M., Gulati, S.C., Clarkson, B.D., 1988. Discordant maturation as the primary biological defect in chronic myelogenous leukemia. Cancer Res. 48 (4), 1035–1041.

Stryckmans, P.A., Debusscher, L., Collard, E., 1977. Cell kinetics in chronic granuclotyci leukaemia (CGL). Clin. Haematol. 6 (1), 21–40.

Sun, J.C., Beven, M.J., 2003. Defective CD8 T cell memory following acute infection without CD4 T cell help. Science 300, 339–342.

Tauchi, T., Ohyashiki, K., 2004. Imatinib mesylate in combination with other chemotherapeutic agents for chronic myelogenous leukemia. Int. J. Hematol. 79 (5), 434–440.

Thijsen, S.F.T., Schuurhuis, G.J., van Oostveen, J.W., Ossenkoppele, G.J., 1999. Chronic mlyeloid leukemia from basics to bedside. Leukemia 13, 1646–1674.

Uzunel, M., Mattsson, J., Brune, M., Johansson, J.-E., Aschan, J., Ringden, O., 2003. Kinetics of minimal residual disease and chimerism in patients with chronic myeloid leukemia after nonmyeloablative conditioning and allogeneic stem cell transplantation. Blood 101 (2), 469–472.

Valmori, D., Dutoit, V., Lienard, D., Lejeune, F., Speiser, D., Rimoldi, D., Cerundolo, V., Dietrich, P.Y., Cerottini, J.C., Romero, P., 2000. Tetramer-guided analysis of TCR beta-chain usage reveals a large repertoire of melan-A-specific CD8+ T cells in melanoma patients. J. Immunol. 165 (1), 533–538.

Villasana, M., Radunskaya, A., 2003. A delay differential equation model for tumor growth. J. Math. Biol. 47, 270–294.

Zorn, E., Wang, K.S., Hochberg, E.P., Canning, C., Alyea, E.P., Soiffer, R.J., Ritz, J., 2002. Infusion of CD4+ donor lymphocytes induces the expansion of CD8+ donor T cells with cytolytic activity directed against recipient hematopoietic cells. Clin. Cancer Res. 8, 2052–2060.